Construction and Building Materials 81 (2015) 172–178

Contents lists available at ScienceDirect

Construction and Building Materials

journal homepage: www.elsevier.com/locate/conbuildmat

Effect of metakaolin on the corrosion resistance of structural lightweight concrete

Oğuzhan Keleştemur *, Bahar Demirel

Technology Faculty, Civil Engineering Department, Firat University, Elazig 23119, Turkey

HIGHLIGHTS

- We investigated the corrosion resistance of SLC specimens with MK at various ratios.
- MK addition improved the physical properties of the SLC specimens.
- Addition of MK in ratios up to 15% w/w improved the mechanical strength of the SLC.
- Use of MK in ratios up to 15% w/w improved the corrosion resistance of the SLC.
- MK higher than 15% w/w reduced the mechanical strength and corrosion resistance.

ARTICLE INFO

Article history:
Received 1 December 2014
Received in revised form 27 January 2015
Accepted 18 February 2015

Keywords:
Metakaolin
Corrosion
Structural lightweight concrete
Microstructure

ABSTRACT

In this study, the mechanical and physical properties of structural lightweight concrete (SLC) specimens produced by substituting cement with metakaolin (MK) at ratios of 5%, 10%, 15% and 20% w/w were examined, and the corrosion behavior of the reinforcing steel bars embedded in these specimens was investigated. Corrosion rates of the bars were determined by using galvanic current measurement method. Furthermore, the corrosion potential of the steel bars in these specimens was measured daily for a period of 90 d based on ASTM C876 standard test method. As a result of this study, it was found that the MK improved the mechanical and physical properties of the SLC and the 15% w/w MK addition showed the optimum contribution to the strength development. Furthermore, the use of MK in SLC specimens, as a cement replacement up to 15% w/w, improved the corrosion resistance of the specimens, while there was no positive effect when MK was added in greater ratios. The conclusions were also supported with scanning electron microscope (SEM) studies.

1. Introduction

During the past decade, metakaolin (MK), a thermally activated amorphous alumina-silicate material acquired by calcining kaolin clay at the temperature range of 750–850 °C, has been objective of several studies, mainly due to its capacity to react vividly with $Ca(OH)_2$ by-products occurred during cement hydration [1,2]. Due to its high pozzolanic activity, the addition of MK greatly enhances the mechanical and durability properties of cement based materials [3–8]. Recent works have shown that MK is a very effective pozzolan, altering the pore structure of the lime and cement paste and greatly improving its resistance to the entrance of water and diffusion of harmful ions through the cement matrix, supporting the idea of its beneficial addition in cement based materials [9–15]. The reaction between the MK and calcium hydroxide (CH) produces tobermorite gel and alumina phases including C_4AH_{13}, C_2ASH_8 and C_3AH_6 at ambient temperature [16]. These phase's stability may lead to dense interfacial transition zone, producing a decrease in porosity and gain of microstructural compactness, i.e., more mechanical and physical strength.

The corrosion resistance of the concrete affects its durability and finally its performance. The durability of reinforced concrete structures is provided by both chemical and physical protection of the reinforcing steel bar against corrosion. Reinforcing steel embedded in good quality concrete normally displays good long-term durability due to the pore solution phase being sufficiently alkaline to lead to passivation of the bar. But, concrete is a porous composite material and thus reinforcing bar protection resulting from the penetration of aggressive ions may not remain excellent long term. This protection depends mainly on the environmental conditions, microstructure and the chemistry of the mixture.

* Corresponding author. Fax: +90 424 2367064.
E-mail address: okelestemur@firat.edu.tr (O. Keleştemur).

http://dx.doi.org/10.1016/j.conbuildmat.2015.02.049
0950-0618/© 2015 Elsevier Ltd. All rights reserved.

The two latter factors are strongly affected by the mix design and quality of its constituents. It is apparent that the existence of MK affects the corrosion resistance of concrete [17,18].

Various studies have been performed on the determining the corrosion behavior of concretes produced with MK. But, not a single study has been encountered on corrosion resistance of SLC obtained by substituting cement with MK in the open literature. Therefore, the aim of this study was to investigate the corrosion behavior of SLC specimens containing MK at proportions of 5%, 10%, 15% and 20% by weight. Furthermore, the mechanical and physical performances of the SLC specimens were also determined.

2. Materials and methods

A total five series of adjacent SLC specimens, including the control specimen, were prepared to determine the effect of MK addition on the corrosion behavior of reinforcing steel embedded in SLC specimens. A total of twenty-five pieces of 100 × 100 × 200 mm concrete specimens consisting of cube specimens in adjacent position were produced, with five specimens being taken from each series. Corrosion rate of the steel bars embedded in these specimens was determined based upon the galvanic current measurement method (GCM).

GCM is based on the principle of determining the galvanic current between electrodes immersed in electrolytes with various contents by using a sensitive ammeter. GCM was applied in two different methods by Jang and Iwasaki [19]. In the first method, out of two electrodes, one was submerged in a solution with broken concrete particles and chloride, the other was submerged in a solution without chloride. These solutions in two different containers were made to come into contact with each other by a saturated ammonium nitrate salt bridge. Electrodes were connected to each other by a cable, and the ratio of current passing through the corrosion cells was measured by means of a sensitive ammeter. The same test was also carried out by using two concrete specimens in lieu of solution containing concrete particles. In this instance, a thin film was placed between the concrete specimens. The specimens were connected to each other by a salt bridge, and galvanic current between the electrodes was measured through the agency of a sensitive ammeter. Keleştemur [20] investigated the corrosion resistance of concrete specimens produced by substituting coarse aggregate with waste vehicle rubber tires at various proportions by using GCM. Asan and Yalçın [21] determined the effects of chloride and acetate ions on the corrosion resistance of concrete containing fly ash by using GCM.

In this study, 5% w/w NaCl was added into the mixing water on one side of the adjacent SLC specimens. In this way, it was considered that galvanic current would occur between the reinforcing steels in the SLC specimens containing MK and with or without NaCl. The galvanic current values were measured daily for a period of 90 days by using a high impedance ammeter. Relative corrosion rates of the electrodes embedded in SLC specimens were determined by dividing galvanic current passing through the galvanic cell to the surface area of the steel.

The corrosion potentials of the electrodes embedded in SLC specimens were determined daily for a period of 90 days based on the ASTM C876 standard test method. The corrosion potentials of the reinforcing steels were measured versus time using a saturated copper/copper sulfate electrode (CSE) as a reference electrode. Corrosion potential measurements were carried out by using a high impedance voltmeter as measurement device. The corrosion potential changes of the steels versus time were showed as graphic to determine whether the electrodes were in active or passive situation.

2.1. Preparing electrodes

The rounded bar of SAE1010 steel produced by Ereğli Iron and Steel Factory in Turkey, which is main material of the construction sector, was chosen for this study as an electrode. The as-received material was in the form of 14 mm in diameter hot-rolled bar. The chemical analysis of the electrode is given in Table 1.

50 pieces of electrodes 120 mm in length were cut out from the as-received material and surfaces of the electrodes were mechanically cleaned with the aid of lathe machine. Then, electrode surfaces were polished with 1200 mesh sandpaper and cleaned with ethyl alcohol. 10 cm^2 surface areas were left open in the tips of steels which would be embedded in the SLC specimens. Screw thread was machined in the other ends of the steels and cables were connected to these ends for make easier measurements in the course of the test. Remaining regions of the steels were covered from exterior effects by coating them with epoxy resin at first and then with polyethylene. The steel bars were kept in a desiccator to protect them against corrosion up to test time.

Table 1
Chemical analysis of the electrode (% wt.).

C	Mn	Si	P	S	Fe
0.17	0.250	0.050	0.005	0.050	Balance

2.2. Preparing SLC specimens for the corrosion tests

100 × 100 × 200 mm SLC specimens consisting of cube blocks in adjacent position were prepared for corrosion tests. Rebars prepared in advance were embedded in these specimens as shown in Fig. 1(a). While one of the blocks contained 5% w/w NaCl, the other one was normal composition. A total of 25 specimens were prepared to determine the corrosion resistance of SLC specimens containing at various proportions of MK. The compositions of the concrete blocks in adjacent position are given in Table 2.

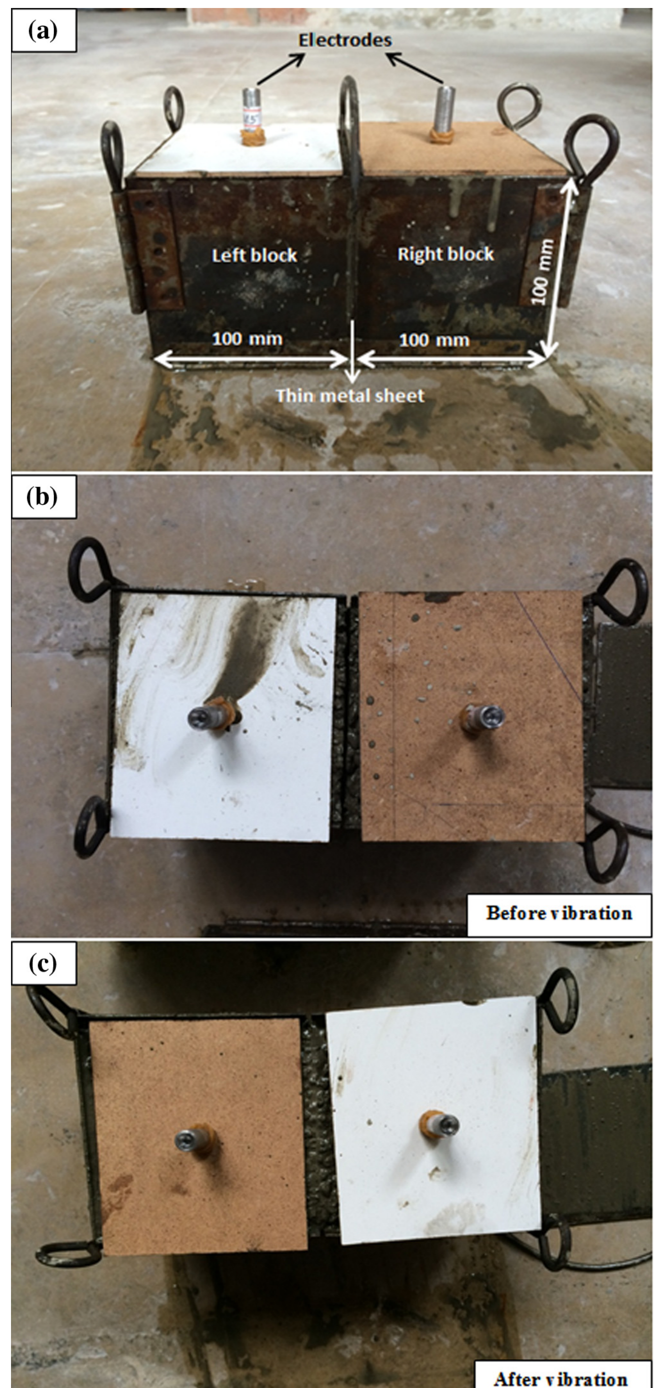

Fig. 1. SLC blocks in adjacent position.

Table 2
Compositions of the adjacent blocks.

Specimen	Left block	Right block
C	Normal mix	Normal mix + 9.5 kg/m^3 Cl^-
M5	Normal mix + 5% w/w MK	Normal mix + 5% w/w MK + 9.5 kg/m^3 Cl^-
M10	Normal mix + 10% w/w MK	Normal mix + 10% w/w MK + 9.5 kg/m^3 Cl^-
M15	Normal mix + 15% w/w MK	Normal mix + 15% w/w MK + 9.5 kg/m^3 Cl^-
M20	Normal mix + 20% w/w MK	Normal mix + 20% w/w MK + 9.5 kg/m^3 Cl^-

The thin metal sheet was placed between the blocks as shown in Fig. 1(a). After the placing of fresh concrete to the blocks, this metal sheet was removed while the concrete was still plastic consistency (Fig. 1(b)). Then, concrete specimens in adjacent position were obtained by applying the vibration to the molds (Fig. 1(c)).

Commercial grade ASTM Type I Portland cement was used to prepare all SLC specimens that were employed in the tests within the scope of this study. MK was obtained from Denge Chemical Company in Turkey. Table 3 compares the chemical and physical properties of the cement and MK used in the mixtures.

High-quality river gravel was used as coarse aggregate which is commonly used in concrete production. Maximum grain size of the coarse aggregate was 8 mm. The density of the river gravel was 2600 kg/m^3. The pumice aggregate with basic character used as fine aggregate (0–4) was provided from the Meryem volcano, placed in Elazig county of Turkey. The density of the basal pumice aggregate was 1850 kg/m^3. The particle size distribution of the aggregate used in this study is given in Table 4. Regular tap water was used as the mixing water period of the preparation of the SLC specimens. Neither plasticizer nor any other chemical admixture was used. The mixture ratios of all the SLC blocks were prepared according to ACI 211.1, and presented in Table 5.

The SLC specimens were kept in molds for period of 24 h at room temperature of about 20 ± 2 °C. After demolding, the specimens were cured at 25 ± 2 °C in 90% relative humidity during the corrosion tests for prevents the specimens from losing their conductive nature.

2.3. Hardened structural lightweight concrete tests

Different tests were performed on the hardened SLC specimens in order to determine their mechanical and physical performances. The mechanical and physical properties such as compressive strength, splitting tensile strength and ultrasonic pulse velocity (UPV) were determined according to ASTM C39, ASTM C496 and ASTM C597, respectively. Furthermore, sorptivity and porosity tests were also carried out on the SLC specimens. The data obtained from mechanical and physical tests were analyzed together with the corrosion data of the SLC specimens.

The porosity of the SLC specimens was measured applying the vacuum-saturation technique. The porosity tests were carried out on slices of 68 mm diameter cores cut out from the center of 100 mm cubes (parallel to the casting direction). The specimens were dried in an oven at 100 ± 5 °C till mass stabilization was reached and were then located in a desiccator under vacuum for at least 3 h, after which the desiccator was filled with de-aired, distilled water. The porosity value for each specimen was calculated through Eq. (1). This porosity measurement technique has previously been reported [22–24].

$$P = \frac{(W_{sat} - W_{dry})}{(W_{sat} - W_{wat})} 100 \qquad (1)$$

where, P stands for vacuum saturation porosity (%); W_{sat} represents weight in air of saturated specimen; W_{wat} represents weight in water of saturated specimen and W_{dry} represents weight of oven-dried specimen.

Five test specimens for capillary sorption test were prepared for each mixture. The capillary sorption tests were performed on 100 mm cube specimens. Tests of sorptivity were conducted using specimens pre-conditioned in the furnace at about 50 °C. After mass stabilization, specimens were sealed by using paraffin on their side surfaces only, for ensure uniaxial water absorption. The end of the specimen that will not be exposed to water was sealed using a loosely attached plastic bag to control evaporation from this surface. The plastic bag was secured using an elastic band. Rods supports were placed at the bottom of the pan and the pan was filled with tap water so that the water level was 5 mm above the top of the rods supports. The water level in the pan was maintained 5 mm above the top of the support for the duration of the tests. The test surface of the specimen was placed on the rods supports as shown in Fig. 2. The mass of the specimens was determined using a balance at certain times, then the ratio of absorbed water was calculated and normalized with respect to the cross-section area of the specimens subjected to the water at certain times such as 0, 5, 10, 20, 30, 60, 180, 360 and 1440 min. The following equation was used in order to calculate the capillary absorption coefficient (k).

Table 3
Chemical and physical properties of the cement and MK.

Oxide compounds (mass%)	CEM I 42.5 N	MK
Silica (SiO_2)	21.12	52–54
Alumina (Al_2O_3)	5.62	41–44
Iron oxide (Fe_2O_3)	3.24	<1.5
Calcium oxide (CaO)	62.94	<0.5
Magnesia (MgO)	2.73	<0.4
Sulfur trioxide (SO_3)	2.30	–
Sodium oxide (Na_2O)	–	<0.1
Potassium oxide (K_2O)	–	<2
Titanium oxide (TiO_2)	–	<1
Density (g/cm^3)	3.15	2.6
Blaine fineness (cm^2/g)	3379	22000

Table 4
Particle size distribution of the aggregate.

Sieve size (mm)	8	4	2	1	0.50	0.25
Passage (%)	100	74	57	31	17	9

Table 5
Details of the SLC mixes (kg/m^3).

Specimen	Water	Cement	MK	Fine aggregate (0–4 mm)	Coarse aggregate (4–8 mm)
C	190	400	–	493	285
M5	190	380	20	493	285
M10	190	360	40	493	285
M15	190	340	60	493	285
M20	190	320	80	493	285

$$\frac{Q}{A} = k\sqrt{t} \qquad (2)$$

where Q stands for the quantity of water absorbed in (cm^3); A the cross-section of specimen in contact with water (cm^2); t time (s) and k the sorptivity coefficient of the specimen (cm/s$^{1/2}$). Q/A was plotted against the square root of time ($\sqrt{t}$) in order to determine the k and then, k was obtained from the slope of the linear relation between Q/A and $\sqrt{t}$. This sorptivity measuring technique has been used in many previous studies [25–28].

The microscopic studies of the SLC specimens were conducted at the Electron Microscopy Laboratory of Firat University by using a Jeol JSM7001F scanning electron microscope.

3. Results and discussion

3.1. Results of mechanical and physical tests performed on hardened specimens

Table 6 presents the data obtained from mechanical and physical tests performed on the hardened SLC specimens at 28th day.

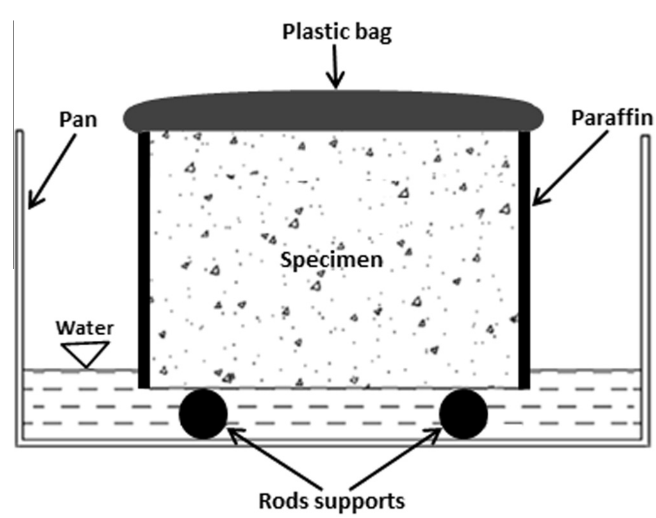

Fig. 2. Schematic demonstration for sorptivity test.

Table 6
Data obtained from mechanical and physical tests.

Tests	Specimens				
	C	M5	M10	M15	M20
Compressive strength (MPa)	29.16	31.86	31.92	36.01	34.34
Splitting tensile strength (MPa)	2.327	2.436	2.637	2.631	2.582
Ultrasonic pulse velocity (km/s)	3.424	3.484	3.572	3.787	3.61
Porosity (%)	11.01	9.35	8.75	3.16	2.91
Sorptivity coefficient $\times 10^{-3}$ (cm/s$^{1/2}$)	1.315	0.994	0.99	0.256	0.201

The compressive and splitting tensile strengths of SLC with MK hydrated for 28 days are shown in Table 6. These results displayed that the compressive and splitting tensile strengths of the SLC specimens increased with the increasing MK replacements up-to 15% w/w. As the case in point, the compressive and splitting tensile strengths of the specimen containing 15% w/w MK were higher than that of the C specimen by about 23.49% and 13.06%, respectively. This gain may have two underlying reasons; the first reason is filler effect of the MK particles in the interface zones between aggregate and cement paste or pores in the bulk paste, thereby enhancing its density as well as its strength. The second reason is pozzolanic reaction, between the MK and $Ca(OH)_2$ released during the cement hydration, which occurs additional $C_3S_2H_3$ gel. The reduction in compressive and splitting tensile strengths for specimen with 20% w/w MK compare to M15 is clarified as the result of dilution effect which reduces the C_3S and βC_2S main phases in blended cement. The dilution effect is a result of substituting a part of cement with the equal amount of MK. At higher ratio replacements, moreover, the MK particles are pelleted around the cement particles and prevent the hydration process. The quantity of hydration productions is reduced; causing to the improvement of fewer points of contact which act as binding centers between cement particles. Therefore, there is an optimum MK replacement for mechanical strength of concrete containing MK. In this study, since the efficiency appears to reduce over a replacement ratio of 15% w/w can also be accepted as an optimum ratio for MK considering the economic efficiency. Similar observations have also been noticed by the other researchers [11,13,16].

The data obtained from UPV tests are given in Table 6. The compressive strength specimens were used for this test. For SLC specimens as the replacement ratio of MK with cement is increased, it behaves to be good soundness properties when compared to C specimen. This observation is found in 5–15% MK only whereas in 20% MK specimen which displayed lesser UPV data compare to 15% MK specimen. From this data it is concluded that the SLC specimen containing up to 15% MK shows to be in a good soundness manner. A similar relationship could be found in the open literature [10].

It is revealed in Table 6 that the porosity and sorptivity coefficient values of the SLC specimens decreased with the rise of MK ratio. This decrease suggested that pore structure of the SLC specimens reduced in accordance with the ratio of MK. The reason of the decreasing of the porosity and sorptivity coefficient values depends on occurring of a denser hydration phase at 28th days. The initial hydration products of Portland cement and MK are $C_3S_2H_3$ gel, C_4AH_{12} and C_2ASH_8 [14,6]. Later on hydrogarnet appears which is denser than C_4AH_{12} and C_2ASH_8. A denser phase is related to reduce in porosity and increase in strength. Furthermore, this decrease in porosity and sorptivity values could be attributed to the filler effect of the fine MK grains. High fineness of MK is expected to yield denser microstructure, in that the MK grains fill the interface zones between the aggregate and cement paste or pores in the matrix. The filler effect can cause discontinuation of the capillary porosity. The beneficial effect of the MK on the decreasing the sorptivity coefficient is obvious when the SLC specimens are visually examined after the end of the sorptivity test. After the experiment has ended, the water can be seen on the top surface of control specimen. As the ratio of MK in the specimens rises the appearance of water on the top surface is greatly decreased. In the SLC specimens produced with 15% and 20% MK at the end of the sorptivity experiment, no water on the top surface is showed. This observation suggests that there is discontinuity of pores when cement is partially replaced with MK. These finding are in good agreement with earlier findings [14,16]. The data obtained from the porosity and sorptivity tests are consistent with the data obtained through mechanical tests.

3.2. Results of corrosion tests

The corrosion tendency of the electrodes was estimated in all types of the SLC specimens by the corrosion potential change versus the test time. Plots of this evolution are presented for the specimens in Fig. 3.

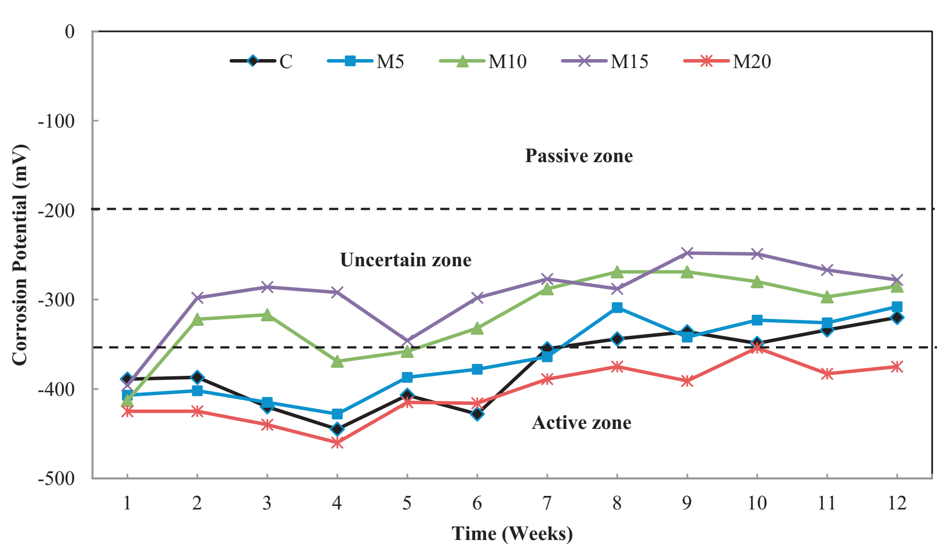

Fig. 3. Changes in corrosion potentials of the specimens.

Recommendations on evaluation of corrosion potential measurement results in ASTM C876 standard test method are given in Table 7 [29].

As seen in Fig. 3, initially the corrosion potentials of almost all electrodes were equal approximately −400 mV. Thereafter recovery was determined to more positive data and finally after 12 weeks of tests it differentiates between the electrodes embedded in various SLC specimens. Fig. 3 presented that the electronegative corrosion potential was much lower in electrodes embedded in SLC specimens containing MK up to 15% w/w compared to the C specimen. Large reduces were determined in electronegative corrosion potential when the MK ratio was raised up to 15%. Indeed, the reinforcing steel bars in the M10 and M15 specimens became more passive than the C specimen and remained in the uncertain zone in terms of corrosion during the 12 weeks period. The corrosion potential of the electrodes embedded in C and M5 specimens had achieved the uncertain zone after the 7th week and remained there during the test. Electrodes in M20 specimen, which poses the highest electronegative corrosion potential, had remained the active zone during the period of test. By taking the ASTM C876 standard as a reference, these results were indicated that the corrosion still continued in M20 specimen even at the end of the 90th day. From the results of corrosion potentials, it can be concluded that the replacement ratio up to 15% MK displayed lower potential values when compared to the C specimen. This phenomenon indicates the influence of the MK on the microstructural diffusion properties of the SLC specimen and also pore size distribution may be reasons for the SLC has significantly decreased the corrosion potential, which acts as filler material.

Table 7
Estimation of corrosion probability as determined by corrosion potential experiment.

Potential (mV), (CSE)	Probability of the presence of active corrosion
>−200	The probability for corrosion is very low
−200 ~ −350	Uncertain
<−350	The probability for corrosion is very high

Corrosion potential tests provide qualitative observations and probably indicate the corrosion of reinforcing bars in concrete to a large extent. Therefore, from the development of corrosion potentials of the reinforcing steels, it is clear that for the first category of specimens a better performance in corrosion resistance is expected than that of second ones.

Among the laboratory experiments, galvanic current measurement versus time provides the ability of a rather correct prediction of a construction service life. Plots of these measurements for all types of the SLC specimens tested are indicated in Fig. 4.

As clearly seen in Fig. 4, the M5, M10 and M15 specimens exhibited developed anticorrosive properties, which cause superior corrosion resistance of the reinforcing steels, whereas M20 presented greater galvanic current value compared to the C specimen. These

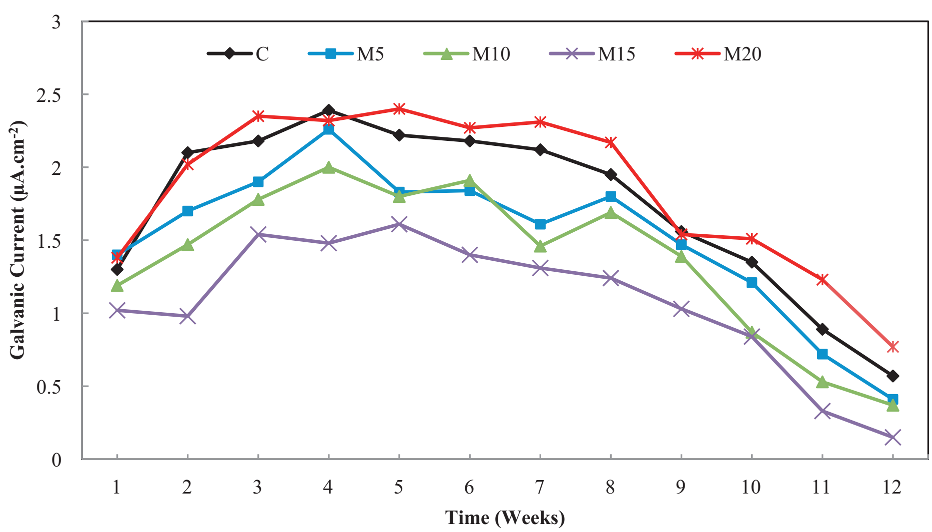

Fig. 4. Changes in the galvanic current values of the specimens.

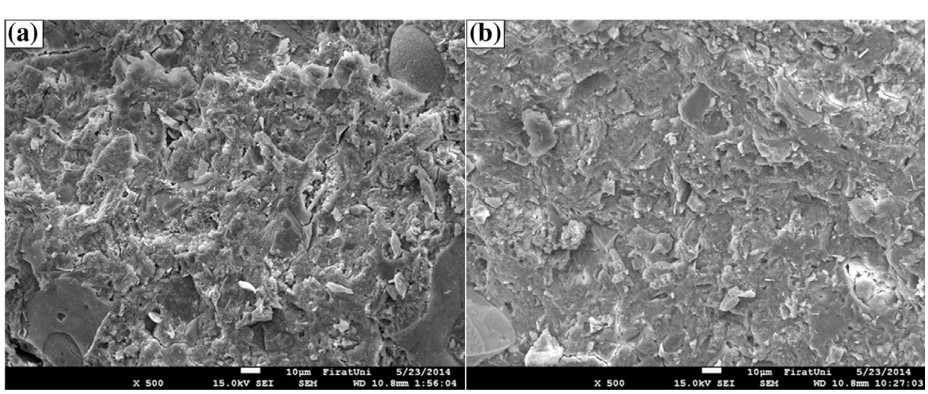

Fig. 5. SEM photographs of SLC specimens: (a) C specimen, (b) M15 specimen.

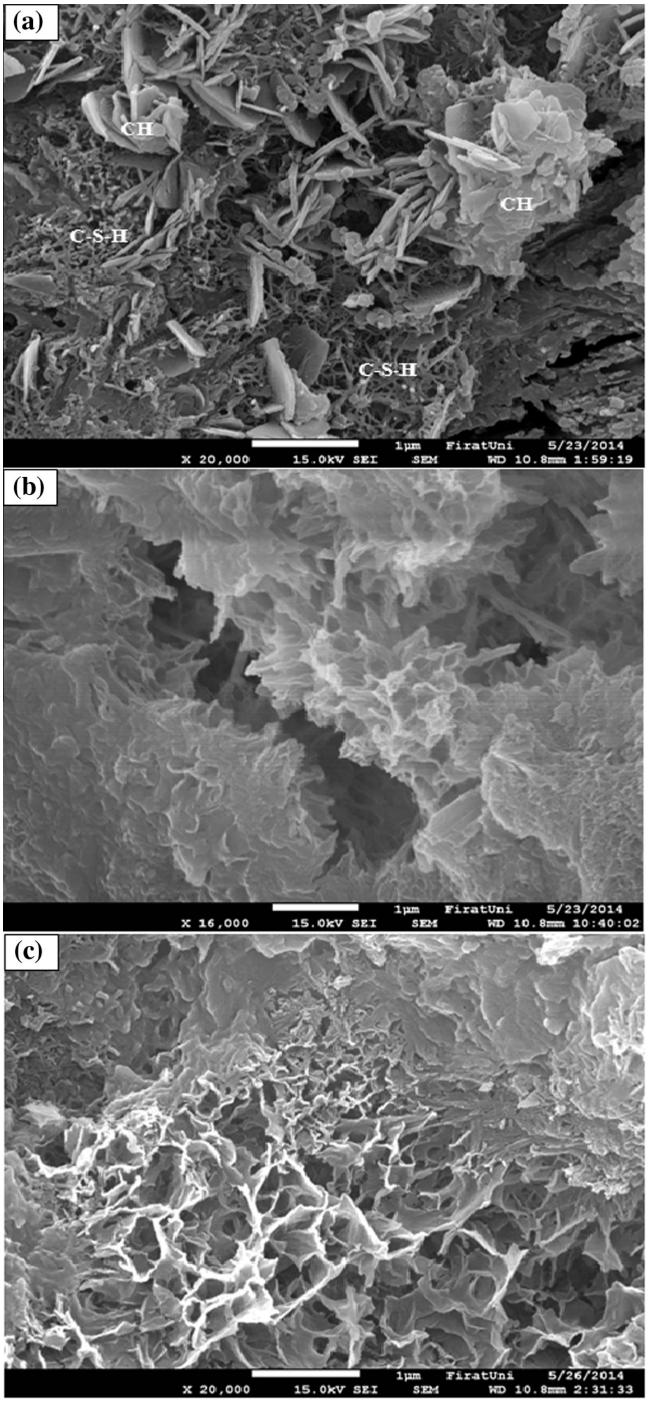

Fig. 6. SEM micrographs of the specimens: (a) C specimen, (b) M15 specimen, (c) M20 specimen.

findings are in consistent with the relevant ones from the corrosion potential tests. Concerning the corrosion, the use of MK, as a cement replacement up to 15% w/w, developed the corrosion resistance of SLC specimens. This rise in corrosion resistance of the specimens could be attributed to denser structure, stronger paste matrix and developed paste-aggregate interface zone of mixtures containing MK as a result of the occur of additional hydrate phases from pozzolanic reaction between the MK and free $Ca(OH)_2$ and its filler effect. The microstructures of the SLC specimens with or without MK at 28th day after hydration are shown in Fig. 5. As shown in Fig. 5, the main structures (separation and irregularity) are improved with addition of the MK. Fig. 5(b) indicated that microstructure of the SCL containing 15% w/w MK is more uniform and dense than that of the C specimen at 28th days. These findings agreed with fairly well with those obtained by other researchers [11,16,18].

Use of MK higher than 15% w/w decreased the corrosion resistance of the SLC specimens. This phenomenon is reasonable considering the reduction of pH degree of the pore solution, because of pozzolanic reaction and following consumption of the calcium hydroxide. The change in the calcium hydroxide content of the specimens with increasing MK ratio is presented in Fig. 6. The SEM micrograph shown in Fig. 6(a) indicates that the microstructure of the C specimen presents the presence of microcrystalline and approximately amorphous C–S–H gels and a large amount of dense calcium hydroxide crystals. Additionally, the micrograph of SLC specimen with 15% MK showed the presence of fibrous and approximately amorphous C–S–H gels and compact microstructure as shown in Fig 6(b). It is clearly seen from Fig. 6(c) that the amount of calcium hydroxide crystals in M20 specimen is decreased. The main reason of this reduction is the pozzolanic reaction between MK and $Ca(OH)_2$ released during cement hydration. The results are in a qualitative agreement with the observations in [11,18,30,31] where were reported that the reduce in the $Ca(OH)_2$ was obvious for concrete specimens containing MK.

The corrosion test data demonstrated that replacement ratio of the 15% w/w shows the best performance among other ratios for corrosion resistance of the SLC specimens produced with MK. This result is in remarkably good agreement with earlier reports [10,18].

4. Conclusions

On the basis of experimental study that has been performed and presented in this study, the following conclusions can be drawn.

- The test results demonstrated that the MK improved compressive and splitting tensile strengths of the SLC specimens and the replacement ratio of 15% w/w MK displayed the optimum contribution to the strength development of the specimens.
- The increase in the ratio of MK resulted in a rise in ultrasonic pulse velocity value of the SLC specimens, but at the same time it lead to reduce in porosity and sorptivity values.
- Incorporation of MK, as a partial cement replacement, into the SLC specimens caused significant changes in the chemical composition of the pore solution phase of the specimens.
- SEM studies revealed that the microstructure of the SLC specimens containing MK up to 15% w/w was more uniform and compact than that of the C specimen.
- As a result of the tests performed for the purpose of determining the corrosion resistance of SLC specimens containing MK at various ratios, it was observed that the use of MK, as a cement replacement up to 15% w/w, improved the corrosion resistance of SLC specimens, while there was no positive effect when MK was added in higher ratio.

References

[1] Changling H, Osbaeck B, Makovicky E. Pozzolanic reaction of six principal clay minerals: activation reactivity assessments and technological effects. Cem Concr Res 1995;25(8):1691–702.
[2] Zhang MH, Malhotra VM. Characteristics of a thermally activated aluminosilicate pozzolanic material and its use in concrete. Cem Concr Res 1995;25(8):1713–25.
[3] Wild S, Khatib JM, Jones A. Relative strength pozzolanic activity and cement hydration in superplasticised MK concrete. Cem Concr Res 1996;26:1537–44.
[4] Frias M, Cabrera J. Pore size distribution and degree of hydration of metakaolin – cement pastes. Cem Concr Res 2000;30:561–9.

[5] Curcio F, DeAngelis BA, Pagliolico S. Metakaolin as a pozzolanic microfiller for high-performance mortars. Cem Concr Res 1998;28:803–9.
[6] De Silva PS, Glasser FP. Hydration of cements based on metakaolin: thermochemistry. Adv Cem Res 1990;3:167–77.
[7] Khatib JM, Wild S. Sulfate resistance of metakaolin mortar. Cem Concr Res 1998;28:120–32.
[8] Larbi JA, Bijen JM. Influence of pozzolans on the Portland cement paste–aggregate interface in relation to diffusion of ions and water absorption in concrete. Cem Concr Res 1992;22:551–62.
[9] Gameiro AL, Silva AS, Veiga MR, Velosa AL. Lime-metakaolin hydration products: a microscopy analysis. Mater Technol 2012;46(2):145–8.
[10] Parande AK, Babu BR, Karthik MA, Deepak Kumaar KK, Palaniswamy N. Study on strength and corrosion performance for steel embedded in metakaolin blended concrete/mortar. Constr Build Mater 2008;22:127–34.
[11] Ramezanianpour AA, Bahrami Jovein H. Influence of metakaolin as supplementary cementing material on strength and durability of concretes. Constr Build Mater 2012;30:470–9.
[12] Khatip JM, Hibbert JJ. Selected engineering properties of concrete incorporating slag and metakaolin. Constr Build Mater 2005;19:460–72.
[13] Kim HS, Lee SH, Moon HY. Strength properties and durability aspects of high strength concrete using Korean metakaolin. Constr Build Mater 2007;21:1229–37.
[14] Khatip JM, Clay RM. Absorption characteristics of metakaolin concrete. Cem Concr Res 2004;34(1):19–29.
[15] Courard L, Darimont A, Schouterden M, Ferauche F, Willem X, Degeimbre R. Durability of mortars modified with metakaolin. Cem Concr Res 2003;33:1473–9.
[16] Siddique R, Klaus J. Influence of metakaolin on properties of mortar and concrete: a review. Appl Clay Sci 2009;43:392–400.
[17] Fajardo G, Valdez P, Pacheco J. Corrosion of steel rebar embedded in natural pozzolan based mortars exposed to chlorides. Constr Build Mater 2009;23:768–74.
[18] Batis G, Pantazopoulou S, Tsivilis S, Badogiannis E. The effect of metakaolin on corrosion behavior of cement mortars. Cem Concr Comp 2005;27:125–30.
[19] Jang W, Iwasaki I. Rebar corrosion under simulated concrete conditions using galvanic current measurements. Corrosion 1991;47(11):875–84.
[20] Keleştemur O. Utilization of waste vehicle tires in concrete and its effect on the corrosion behavior of reinforcing steels. Int J Miner Metall Mater 2010;17(3):363–70.
[21] Asan A, Yalçın H. Effect of fly ashes on the corrosion of reinforcing steels. Gazi Univ J Sci 2003;16(1):47–54.
[22] Mydin MAO. Modeling of transient heat transfer in foamed concrete slab. J Eng Sci Technol 2013;8(3):326–43.
[23] Cabrera JG, Lynsdale CJ. A new gas permeameter for measuring the permeability of mortar and concrete. Mag Concr Res 1988;40(144):177–82.
[24] Gonen T, Yazicioglu S. The influence of mineral admixtures on the short and long-term performance of concrete. Build Environ 2007;42:3080–5.
[25] Gonen T, Yazicioglu S. The influence of compaction pores on sorptivity and carbonation of concrete. Constr Build Mater 2007;21:1040–5.
[26] Tasdemir C. Combined effects of mineral admixtures and curing conditions on the sorptivity coefficient of concrete. Cem Concr Res 2003;33:1637–42.
[27] Turkmen I. Influence of different curing conditions on the physical and mechanical properties of concretes with admixtures of silica fume and blast furnace slag. Mater Lett 2003;57(29):4560–9.
[28] Demirel B, Keleştemur O. Effect of elevated temperature on the mechanical properties of concrete produced with finely ground pumice and silica fume. Fire Saf J 2010;45:385–91.
[29] ASTM C876–91. Standard test method for half-cell potentials of uncoated reinforcing steel in concrete. Annual Book of ASTM Standards. vol. 4.02. Philadelphia, USA; 1991.
[30] Morsy MS, Al-Salloum YA, Abbas H, Alsayed SH. Behavior of blended cement mortars containing nano-metakaolin at elevated temperatures. Constr Build Mater 2012;35:900–5.
[31] Seleem HEH, Rashad AM, El-Sabbagh BA. Durability and strength evaluation of high performance concrete in marine structures. Constr Build Mater 2010;24(6):878–84.